Chinese Chemical Letters 33 (2022) 948–952

Contents lists available at ScienceDirect

Chinese Chemical Letters

journal homepage: www.elsevier.com/locate/cclet

Highly efficient degradation of emerging contaminants by magnetic $CuO@Fe_xO_y$ derived from natural mackinawite (FeS) in the presence of peroxymonosulfate

Ruohan Zhang[a], Maolian Chen[b], Zhaokun Xiong[a,c,*], Yong Guo[b], Bo Lai[a,c,*]

[a] State Key Laboratory of Hydraulics and Mountain River Engineering, College of Architecture and Environment, Sichuan University-Pittsburgh Institute, Sichuan University, Chengdu 610207, China
[b] Department of Process Equipment and Safety Engineering, School of Chemical Engineering, Sichuan University, Chengdu 610065, China
[c] Sino-German Centre for Water and Health Research, Sichuan University, Chengdu 610065, China

ARTICLE INFO

Article history:
Received 31 May 2021
Revised 4 July 2021
Accepted 9 July 2021
Available online 16 July 2021

Keywords:
Emerging organic contaminants
Mackinawite
Peroxymonosulfate
$CuO@Fe_xO_y$
Reactive oxygen species

ABSTRACT

In this study, natural mackinawite (FeS), a chalcophilic mineral, was utilized to prepare iron/copper bimetallic oxides ($CuO@Fe_xO_y$) by displacement plating and calcination process. Various characterization methods prove that Cu^0 is successfully coated on the surface of FeS, which were further oxidized to CuO, Fe_3O_4 and/or Fe_2O_3 during calcination process, respectively. $CuO@Fe_xO_y$ performed highly efficient capacity to activate PMS for the degradation of various emerging pollutants including sulfamethoxazole (SMX), carbamazepine (CBZ), bisphenol A (BPA), 2,4-dichlorophenol (2,4-DCP) and diclofenac (DCF) in aqueous solution. Complete removal of the above pollutants was observed after 8 min of $CuO@Fe_xO_y$/PMS treatment. Taking SMX as an example, the key parameters including $CuO@Fe_xO_y$ dosage, PMS dosage and initial pH were optimized. The results show that the catalytic system can be worked in a wide pH range (3.0-9.0). The quenching experiments and electron spin resonance (ESR) test demonstrated that the main reactive oxygen species in $CuO@Fe_xO_y$/PMS system were hydroxyl radicals ($^{\bullet}OH$) and sulfate radicals ($SO_4^{\bullet-}$), and $SO_4^{\bullet-}$ was the primary reactive species. Besides, the influence of coexisting anions (*i.e.*, Cl^-, NO_3^-, HCO_3^- and $H_2PO_4^-$) for the degradation of SMX was explored. $CuO@Fe_xO_y$/PMS system can maintain good catalytic activity and reusability in different water bodies and long-term running. This work provided a green strategy to fabricate the efficient catalyst in PMS-based advanced oxidation processes.

The health and environmental problems caused by antibiotic abuse have become a consensus. In recent years, tetracyclines, sulfonamides and quinolones have been detected in surface water, groundwater, drinking water and effluent from sewage treatment plants [1,2]. Antibiotic pollutants have the characteristics of difficult biodegradation, strong biological toxicity, easy to cause bacterial resistance and resistance genes. Sulfamethoxazole (SMX), as a typical sulfonamide antibiotic, has been widely used for the treatment of veterinary disease, respiratory tract, urinary tract infection, and other diseases. Although it has low concentration in the actual environment, it will exist for a long time and accumulate continuously, which are harmful to water environment and human health [3–5]. How to scientifically and effectively remove environmental residual antibiotics has become a key problem to be solved.

Advanced oxidation processes (AOPs) have shown outstanding ability in the treatment of organic pollution wastewater [6–8]. Among diverse AOPs, sulfate radicals based-advanced oxidation processes (SR-AOPs) are proverbial to generate hydroxyl radicals ($^{\bullet}OH$) and sulfate radicals ($SO_4^{\bullet-}$) by persulfate activation [9,10]. Previous works have found that some transition metals (Fe, Co, Ni, Mn and Cu) and their metal oxides (Co_3O_4, Fe_3O_4, CuO, $CoFe_2O_4$ and $CuFe_2O_4$) could tellingly activate persulfate to generate $SO_4^{\bullet-}$ [11–14]. However, the active sites in the heterogeneous catalyst are easily encapsulated inside the catalyst, resulting in lower catalytic activity. Besides, the unavoidable leaching of toxic metal ions from heterogeneous catalysts is also the major drawback in SR-AOPs.

Recently, natural minerals enriched in transition metals as heterogeneous activators have gained increasing attention in water treatment due to their abundant, low cost and widespread source [15–17]. Natural mackinawite is a non-toxic mineral that can be

* Corresponding authors at: State Key Laboratory of Hydraulics and Mountain River Engineering, College of Architecture and Environment, Sichuan University-Pittsburgh Institute, Sichuan University, Chengdu 610207, China.
E-mail addresses: scuxzk@scu.edu.cn (Z. Xiong), laibo@scu.edu.cn (B. Lai).

https://doi.org/10.1016/j.cclet.2021.07.029
1001-8417/

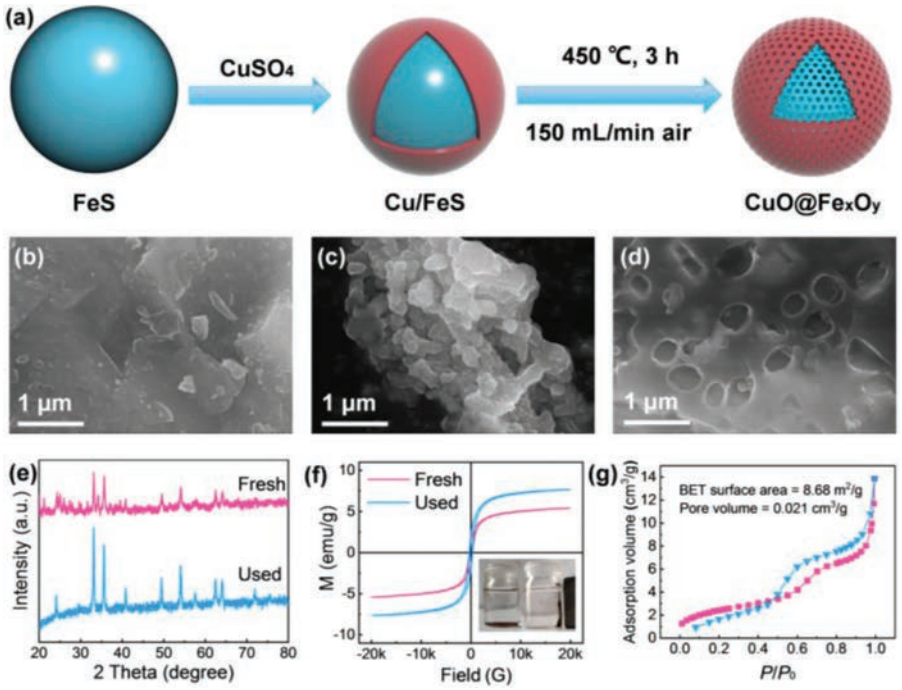

Fig. 1. (a) Schematic illustration of the preparation process of CuO@Fe_xO_y. SEM images of (b) pristine FeS, (c) Cu/FeS, and (d) CuO@Fe_xO_y; (e) the XRD patterns and (f) the magnetic hysteresis loop, (g) N_2 adsorption-desorption isotherms of CuO@Fe_xO_y.

as the precursor with abundance to the more stable iron sulfide minerals [18,19]. Natural mackinawite is mainly composed of iron sulfide (FeS) and has long-term stability in anoxic sediments. Due to the chalcophilic nature, FeS can capture many divalent metals through forming surface complexes [18]. Inspired by this characteristic, Cu^0 can be coated on the surface of FeS particles to form core-shell structure. After calcination process in air atmosphere, Cu^0 on the surface can be oxidized to CuO with high catalytic activity. FeS inside the core is decomposed, and SO_2 escapes from the core and leaves pores on the catalyst to form a porous structure Eqs. 1 and 2. In this study, natural mackinawite was utilized to prepare iron/copper bimetallic oxides by displacement plating and calcination process to activate PMS for the degradation of emerging contaminants in aqueous solution.

$$4FeS + 7O_2 \rightarrow 2Fe_2O_3 + 4SO_2 \quad (1)$$

$$3FeS + 5O_2 \rightarrow Fe_3O_4 + 3SO_2 \quad (2)$$

As shown in Fig. 1a, the CuO@Fe_xO_y particles were prepared by displacement plating with Cu^{2+} and calcination process in air atmosphere. Scanning electron microscope (SEM) image of raw FeS clearly shows that the surface of the material is smooth and free of pores (Fig. 1b). The material presents irregular particle shape when Cu loading on the surface of FeS (Fig. 1c). However, as shown in Fig. 1d, it is observed that there are a lot of pores on the surface of CuO@Fe_xO_y particles, which indicates that a good core-shell structure with pores has been successfully prepared.

The crystalline phases and chemical structures of CuO@Fe_xO_y particles were determined by X-ray diffraction (XRD). As shown in Fig. 1e, the diffraction peak at 35.7° is corresponding to the 111 crystal plane compared with the standard card of CuO (JCPDS No. 44–0706) [20], indicating that CuO has successfully covered on the surface of Fe_xO_y. The diffraction peaks at 24.38° and 33.15° correspond to the 104 and 110 crystal planes of Fe_2O_3. The XRD results of 35.7° and 62.9° correspond to the 311 and 440 crystal planes of Fe_3O_4 [21]. The valence states of CuO@Fe_xO_y were measured by X-ray photoelectron spectroscopy (XPS) and shown in Fig. S1 (Supporting information). The detailed scan of Cu 2p displays that element Cu in CuO@Fe_xO_y mainly exists in form of CuO, and the valence states remained unchanged during the reaction, which proves that the activation of PMS by CuO was a catalytic reaction (Fig. S1b) [22]. The peaks at 710.9 and 724.4 eV correspond to Fe $2p_{3/2}$ and Fe $2p_{1/2}$ of Fe_3O_4 while the peak at 713.4 eV relating to Fe $2p_{3/2}$ of Fe_2O_3 [11], indicating the iron on the surface of FeS particles in CuO@Fe_xO_y is oxidized to a certain extent, and the used catalyst of Fe(III) on the surface of Fe 2p is partially converted to Fe(II) (Fig. S1c). In summary, the CuO@Fe_xO_y catalyst has been successfully prepared. The magnetic properties of CuO@Fe_xO_y are verified by M-H curve analysis, and the results are shown in Fig. 1f. The M-H curve reflects the saturation magnetization of CuO@Fe_xO_y before and after the reaction is about 5.4 emu/g and 7.6 emu/g, respectively. In addition, the inset image of Fig. 1f shows that the CuO@Fe_xO_y was quickly attracted by the external magnet to achieve excellent magnetic separation performance, which is conducive to the recovery and recycling of the catalyst.

The surface area and pore-size distribution of CuO@Fe_xO_y were analyzed by Brunauer-Emmett-Teller (BET) measurements (Fig. 1g). The result indicates that specific surface area of CuO@Fe_xO_y is 8.68 m^2/g. In summary, the porous structure of the catalyst can provide more active sites. The pollutants and oxidant molecules can easily adhere to the surface and smoothly diffuse into the pores, which is beneficial to promote the catalytic process [23].

The SMX removal efficiencies in different systems are illustrated in Fig. 2a. It can be observed that negligible removal of SMX was performed in sole CuO@Fe_xO_y, sole PMS, Fe_3O_4/PMS and Fe_2O_3/PMS systems. While CuO can catalyze PMS to remove about 40% of SMX, surprisingly, CuO@Fe_xO_y performed highly efficient activation of PMS for the degradation of SMX. Completely SMX removal was achieved in the case of CuO@Fe_xO_y/PMS system. Fig. S2 (Supporting information) also shows that the k_{obs} of CuO@Fe_xO_y/PMS system was 0.778 min^{-1}, which was much higher than those of control systems. Besides, the leached

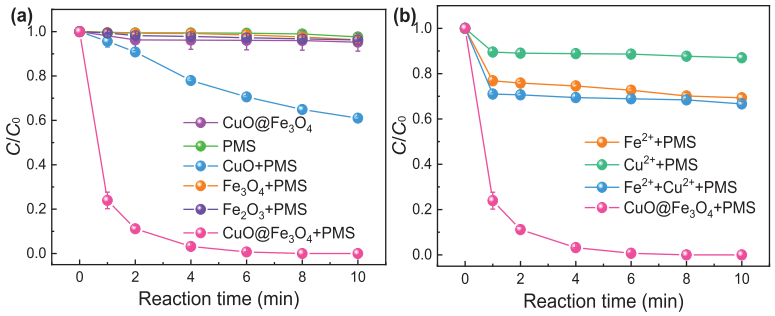

Fig. 2. Degradation efficiency of SMX in different systems. The concentration of metal ions in homogeneous reaction process is the same as that of leached metal ions. Experiment conditions: [catalyst] = 0.3 g/L, $[PMS]_0$= 0.3 mmol/L, $[SMX]_0$= 5 mg/L, solution pH 6.5.

concentrations of metal ions were also monitored in this process. The result illustrates that only 0.15 mg/L of iron ions and 1.21 mg/L of copper ions were leached in CuO@Fe_xO_y/PMS system, respectively. Therefore, the homogeneous catalytic reactions of metal ions were also determined by using the same concentration of leaching metal concentrations. It can be seen from Fig. 2b that the degradation efficiency of SMX by Fe^{2+}/PMS is about 27%, which is higher than that of Cu^{2+}/PMS system (about 10%). The removal rate of Fe^{2+}/Cu^{2+}/PMS system (about 30%) on SMX is only slightly higher than that of Cu^{2+}/PMS. The above results indicated that heterogeneous CuO@Fe_xO_y performed highly efficient to activate PMS for SMX degradation.

The effects of key parameters were also evaluated including catalyst dosage, PMS dosage and initial pH. As shown in Fig. S3 (Supporting information), with the increase of the catalyst dosage, a significant increase in SMX degradation can be observed. The degradation rate rapidly increases to 100% within 8 min in CuO@Fe_xO_y/PMS system as the catalyst dosage gradually increases to 0.3 g/L. A high concentration of catalyst can achieve the purpose of rapid degradation of SMX. Besides, when the PMS concentration increased from 0.05 mmol/L to 0.30 mmol/L, the SMX removal was positively correlated with the PMS concentration, and the degradation rate of SMX increased from 32% to 100% (Fig. S4 in Supporting information). Compared to Mn-based bimetallic oxides which are also used to degrade some emerging organic contaminants in the presence of PMS. Mn-Fe layered double oxides and amorphous MnO_2 *in-situ* anchored titanate nanotubes have lower removal efficiency compared with CuO@Fe_xO_y. It takes approximately 20-30 min for them to get fully degradation [24–26]. Besides, some advanced Co-based materials/PMS systems like h-$Co(OH)_2$/PMS and CoM/TNTs0.5/PMS also cannot achieve complete removal of pollutants within 8 min [24,27,28]. However, when the dosage of PMS increase to 0.40 mmol/L, the degradation efficiency of SMX was significantly inhibited, and the degradation rate of SMX was only about 90% after 10 min of reaction. The reason for the inhibition of degradation may be that PMS preferentially consumes the free radicals generated in the system, resulting in the decline of degradation efficiency. Finally, solution pH was also investigated in CuO@Fe_xO_y/PMS system. It can be seen from Fig. S5 (Supporting information) that CuO@Fe_xO_y/PMS system can achieve a good degradation efficiency on SMX (above 90%) when the initial pH is in the range of 3.0-6.5. However, the degradation process of SMX is slightly inhibited when the pH is alkaline. The reason for the inhibitory effect under alkaline conditions is that the electrostatic repulsion between CuO@Fe_xO_y and PMS is strengthened, thus hindering the contact between the catalyst and PMS and the target pollutants, and further hindering the mass transfer process. Overall, CuO@Fe_xO_y/PMS system has a wide pH tolerance range in the range of 3.0-9.0, which shows that this process has great engineering application potential. After comprehensive consideration, the initial pH of the original SMX solution without any adjustment (pH 6.5) was selected in the subsequent experiments. As Fig. S6 (Supporting information) shows, the final pH ranges from 3.07 to 4.95 based on different reaction systems.

In addition, the investigation on interferences of inorganic anions for SMX degradation in CuO@Fe_xO_y/PMS system was performed. It can be seen from Fig. S7 (Supporting information) that Cl^- shows a significant promotion effect for SMX removal when the concentration of Cl^- is between 0 and 5 mmol/L in CuO@Fe_xO_y/PMS system. Previous studies have shown that the impact of Cl^- on the degradation of pollutants in AOPs is very complex. Cl^- can react with PMS through electron transfer reactions to generate more oxidative HOCl [29,30]. Wang *et al.* proved through experiments that HOCl alone can directly oxidize SMX [24]. It also preliminarily verified that the free radical pathway may be followed in the degradation of oxidative SMX in this study. Moreover, NO_3^- with various concentrations showed slightly inhibitory effects on SMX degradation (Fig. S8 in Supporting information). NO_3^- reacts with free radicals to produce $NO_3^{\bullet}$, which has a weak oxidizing capacity. The degradation rate of pollutants is inhibited due to the consumption of free radicals. It can be seen from Fig. S9 (Supporting information) that distinct inhibitory effects are observed in the presence of HCO_3^-. HCO_3^- quickly reacts with $SO_4^{\bullet-}$ and $^{\bullet}OH$ to produce $CO_3^{\bullet}$ with lower oxidability. On the other hand, HCO_3^- can increase the solution pH to the alkaline condition, which would be a negative impact on SMX removal. Furthermore, an apparent inhibition was also observed even if 5 mmol/L of $H_2PO_4^-$ was added into the solution (Fig. S10 in Supporting information). The main reason is that $H_2PO_4^-$ reacts with $SO_4^{\bullet-}$ and $^{\bullet}OH$ to consume the active substances as a free radical quencher, which inhibits the degradation of pollutants. Moreover, $H_2PO_4^-$ can form complex with Fe-based catalyst due to the affinity of $H_2PO_4^-$ with active sites on the catalyst surface, resulting in the decline of degradation rate of SMX.

Scavenging experiments in various initial pH conditions were conducted to gain insight into the degradation mechanism [11]. As shown in Fig. 3a, the degradation rate of SMX was suppressed to 65% when 0.1 mol/L TBA was added to the system. It can be concluded that $^{\bullet}OH$ was involved in CuO@Fe_xO_y/PMS system**.** However, the degradation of SMX was almost completely inhibited in the presence of 0.1 mol/L EtOH. This result demonstrated that both $^{\bullet}OH$ and $SO_4^{\bullet-}$ contributed to the degradation of SMX in CuO@Fe_xO_y/PMS system**.** Furthermore, similar inhibitory effects were observed in both acidic and alkaline conditions when TBA and EtOH were introduced in CuO@Fe_xO_y/PMS system at initial pH of 3.0 and 9.0. By comparing the suppressive efficiencies in various initial conditions, it can be concluded that the primary reactive species was $SO_4^{\bullet-}$.

To further verify the main reactive oxygen species (ROS) in the CuO@Fe_xO_y/PMS system, 5,5-dimethyl-1-pyrrolidine-*N*-oxide

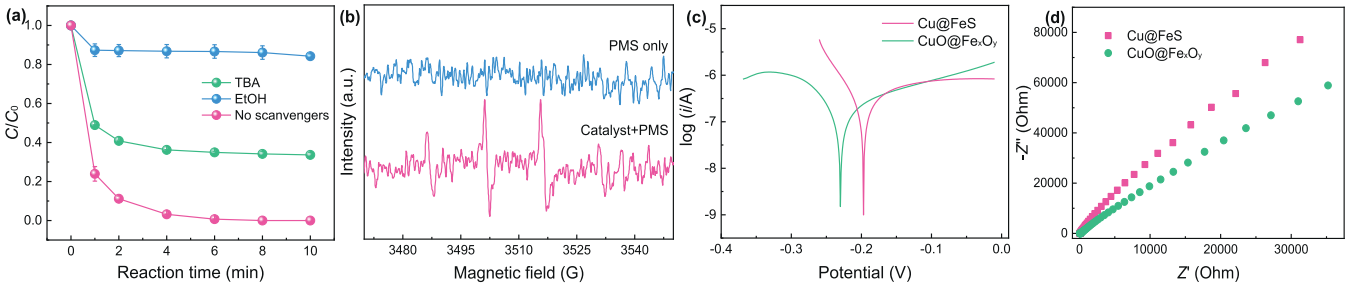

Fig. 3. (a) Effects of different radical scavengers for the SMX degradation in CuO@Fe_xO_y/PMS system at initial pH of 6.5. (b) ESR spectra in CuO@Fe_xO_y/PMS system with DMPO as the trapping agent. (c) Tafel polarization curves and (d) electrochemical impedance spectroscopic analysis of CuO@Fe_xO_y and Cu@FeS. Experiment conditions: [catalyst] = 0.3 g/L, $[PMS]_0$= 0.3 mmol/L, $[SMX]_0$= 5 mg/L, TBA = EtOH = 0.1 mol/L, solution pH 6.5.

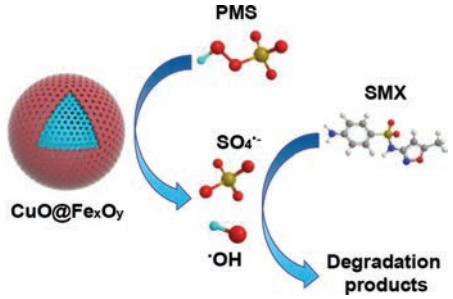

Fig. 4. The possible degradation mechanisms of SMX in CuO@Fe_xO_y/PMS system.

(DMPO) as spin-trapping agent was utilized in electron spin resonance (ESR) determination. Fig. 3b clearly showed that a typical 1:2:2:1 four-peak of DMPO-OH adduct (α_N = 14.9 G, α_H = 14.9 G) was detected in ESR spectrum, which illustrated •OH is indeed generated during the catalytic oxidation of the system. However, the signal of DMPO-SO_4 is not shown in Fig. 3b. $SO_4^{\bullet-}$ is easy to react with water to transfer into •OH. Besides, DMPO-SO_4 adducts are prone to nucleophilic substitution reactions and converted to DMPO-OH. Furthermore, electrochemical measurements were adopted by using Tafel and electrochemical impedance spectroscopy (EIS) to verify the electron migration rate of CuO@Fe_xO_y and Cu@FeS. Tafel and EIS analysis both indicated that CuO@Fe_xO_y performed higher electron transfer rate and better catalytic activity compared to Cu@FeS (Fig. 3c and d). This phenomenon can be attributed to the high conductivity of bimetallic oxide that can accelerate the charge transfer [14,31]. According to the above experiments and analysis, the possible degradation mechanism of SMX in CuO@Fe_xO_y/PMS system is illustrated in Fig. 4.

Additionally, SMX degradation efficiencies in different water bodies are depicted in Fig. 5a. A slight drop of degradation efficiency was observed in tap water and Yangtze River water. But SMX can be also completely removed within 10 min. In terms of the overall effect, the CuO@Fe_xO_y/PMS system showed excellent catalytic oxidation capacity in different water bodies. It can be seen from Fig. 5b that carbamazepine (CBZ), bisphenol A (BPA), 2,4-dichlorophenol (2,4-DCP) and diclofenac (DCF) can be completely removed within 8 min in CuO@Fe_xO_y/PMS system. Therefore, the CuO@Fe_xO_y/PMS process has great application prospects in the degradation of various emerging pollutants. Finally, five consecutive experiments of SMX degradation were conducted to evaluate the long-term efficiency of CuO@Fe_xO_y/PMS system. Fig. 5c shows the degradation efficiencies of SMX in five consecutive experiments by replacing the reactive solution of each cycle. The result indicated that CuO@Fe_xO_y/PMS system performed satisfactory reusability during long-term running (*e.g.*, completely degradation of SMX was performed within 10 min after the fifth cycle). However, the degradation efficiencies of SMX gradually declined when remained the solution and only add 5 mg/L of SMX after each consecutive experiment (Fig. 5d) [32,33]. The accumulation of degradation intermediates can consume the ROS during consecutive experiments, and then declined the removal rate of SMX in this circumstance. Anyway, the results of cyclic experiments demonstrated that CuO@Fe_xO_y/PMS system performed good activity for long-term running.

In summary, CuO@Fe_xO_y bimetallic oxides were fabricated by using chalcophilic natural mackinawite as the precursor. Various characterization methods prove that CuO was successfully coated on the surface of Fe_xO_y. It is also found that there were abundant mesoporous structures on the surface of catalyst, which further enhances the catalytic performance for PMS activation. CuO@Fe_xO_y has a much higher ability to activate PMS for the degradation of SMX. Scavenging experiments and ESR analysis indicated that both •OH and $SO_4^{\bullet-}$ contributed to the degradation of SMX, and $SO_4^{\bullet-}$ was the primary reactive species. Different types of emerging pol-

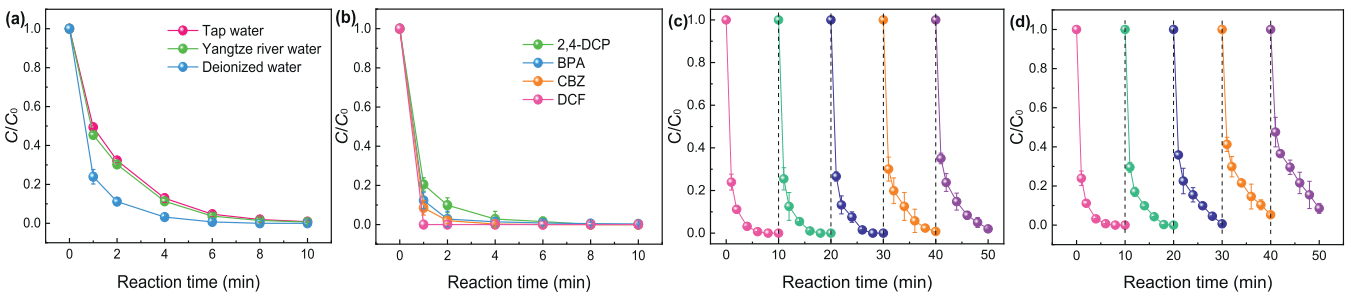

Fig. 5. (a) Degradation of SMX by CuO@Fe_xO_y/PMS in the presence of actual waterbody, (b) removal efficiencies of various pollutants in CuO@Fe_xO_y/PMS system. The long-term efficiencies of (c) replacing the solution, (d) remains the solution and only add a certain amount of SMX after each consecutive experiment by CuO@Fe_xO_y/PMS system.

lutants can be efficiently degraded by CuO@Fe_xO_y/PMS system. The excellent magnetic properties are conducive to the recycling of the catalyst and performed satisfactory reusability during long-term running.

Declaration of competing interest

The authors declare that they have no known competing financial interests or personal relationships that could have appeared to influence the work reported in this paper.

Acknowledgments

The authors would like to acknowledge the financial support from National Natural Science Foundation of China (No. 51878423), China Postdoctoral Science Foundation (No. 2019T120843), and Sichuan Science and Technology Program (No. 2019YJ0091).

Supplementary materials

Supplementary material associated with this article can be found, in the online version, at doi:10.1016/j.cclet.2021.07.029.

References

[1] Q.Q. Zhang, G.G. Ying, C.G. Pan, Y.S. Liu, J.L. Zhao, Environ. Sci. Technol. 49 (2015) 6772–6782.
[2] H. Wang, J. Yang, X. Yu, et al., Environ. Sci. Technol. 52 (2018) 13942–13950.
[3] Y. Li, J. Li, Y. Pan, et al., Chem. Eng. J. 384 (2020) 123361.
[4] S. Nimai, H. Zhang, Z. Wu, N. Li, B. Lai, Chin. Chem. Lett. 31 (2020) 2657–2660.
[5] M. Feng, J.C. Baum, N. Nesnas, et al., Environ. Sci. Technol. 53 (2019) 2695–2704.
[6] J. Li, Y. Li, Z. Xiong, G. Yao, B. Lai, Chin. Chem. Lett. 30 (2019) 2139–2146.
[7] H. Zhang, Q. Ji, L. Lai, G. Yao, B. Lai, Chin. Chem. Lett. 30 (2019) 1129–1132.
[8] B. Huang, Z. Wu, H. Zhou, et al., J. Hazard. Mater. 412 (2021) 125253.
[9] Z. Xiong, Y. Jiang, Z. Wu, G. Yao, B. Lai, Chem. Eng. J. 421 (2021) 127863.
[10] J. Wang, S. Wang, Chem. Eng. J. 334 (2018) 1502–1517.
[11] Z. Wu, Y. Wang, Z. Xiong, et al., Appl. Catal. B: Environ. 277 (2020) 119136.
[12] J. Li, M. Xu, G. Yao, B. Lai, Chem. Eng. J. 348 (2018) 1012–1024.
[13] J. Li, J. Yan, G. Yao, et al., Chem. Eng. J. 361 (2019) 1317–1332.
[14] Y. Lei, C.S. Chen, Y.J. Tu, Y.H. Huang, H. Zhang, Environ. Sci. Technol. 49 (2015) 6838–6845.
[15] J. Peng, H. Zhou, W. Liu, et al., Chem. Eng. J. 397 (2020) 125387.
[16] L. Lai, H. Zhou, B. Lai, Chem. Eng. J. 349 (2018) 633–645.
[17] L. Lai, H. Ji, H. Zhang, et al., Appl. Catal. B: Environ. 282 (2021) 119559.
[18] D. Cheng, S. Yuan, P. Liao, P. Zhang, Environ. Sci. Technol. 50 (2016) 11646–11653.
[19] Y. Gong, J. Tang, D. Zhao, Water Res. 89 (2016) 309–320.
[20] Y. He, J. Zhang, H. Zhou, G. Yao, B. Lai, Chem. Eng. J. 380 (2020) 122568.
[21] Y. Dai, L. Niu, J. Zou, et al., Chin. Chem. Lett. 29 (2018) 887–891.
[22] F. Ji, C. Li, L. Deng, Chem. Eng. J. 178 (2011) 239–243.
[23] Y. Zhu, Z.-S. Bai, H.-L. Wang, Chin. Chem. Lett. 28 (2017) 633–641.
[24] S. Wang, L. Xu, J. Wang, Chem. Eng. J. 375 (2019) 122041.
[25] L. Li, Q. Zhang, Y. She, Y. Yu, J. Hong, Sep. Purif. Technol. 270 (2021) 118770.
[26] F. Pan, H. Ji, P. Du, et al., J. Hazard. Mater. 402 (2021) 123779.
[27] L. Chen, H. Ji, J. Qi, et al., Chem. Eng. J. 406 (2021) 126877.
[28] M. Ma, L. Chen, J. Zhao, W. Liu, H. Ji, Chin. Chem. Lett. 30 (2019) 2191–2195.
[29] R. Luo, M. Li, C. Wang, et al., Water Res. 148 (2019) 416–424.
[30] F. Chen, L.L. Liu, J.J. Chen, et al., Water Res. 191 (2021) 116799.
[31] T. Sun, Z. Zhao, Z. Liang, et al., Chem. Eng. J. 334 (2018) 1527–1536.
[32] Z. Xiong, J. Li, Y. Li, et al., J. Hazard. Mater. 406 (2021) 124725.
[33] X. Wang, X. Pu, Y. Yuan, et al., Chin. Chem. Lett. 31 (2020) 2634–2640.